INTERNATIONAL JOURNAL OF
NUMERICAL ANALYSIS AND MODELING
Volume 18, Number 1, Pages 19–37

LOCALLY CONSERVATIVE SERENDIPITY FINITE ELEMENT SOLUTIONS FOR ELLIPTIC EQUATIONS

YANHUI ZHOU AND QINGSONG ZOU

Abstract. In this paper, we post-process an eight-nodes-serendipity finite element solution for elliptic equations. In the post-processing procedure, we first construct a *control volume* for each node in the serendipity finite element mesh, then we enlarge the serendipity finite element space by adding some appropriate element-wise bubbles and require the novel solution to satisfy the local conservation law on each control volume. Our post-processing procedure can be implemented in a parallel computing environment and its computational cost is proportional to the cardinality of the serendipity elements. Moreover, both our theoretical analysis and numerical examples show that the postprocessed solution converges to the exact solution with optimal convergence rates both under H^1 and L^2 norms. A numerical experiment for a single-phase porous media problem validates the necessity of the post-processing procedure.

Key words. Postprocessing, serendipity finite elements, local conservation laws, error estimates.

1. Introduction

The serendipity family of finite elements is one of the most popular finite element methods (FEMs) applying parallelepiped meshes. Over each such a mesh, the serendipity finite element space with C^0 continuity has significantly smaller dimension than the alternative tensor product Lagrange element space, yet they have the same convergence orders. With this advantage and others, the serendipity finite elements have been studied by many researchers such as Ahmad [1] in 1969, Zienkiewicz [41] in 1977, Macneal and Harder [26] in 1992, Lee and Bathe [17] in 1993, Kikuchi [15] in 1994, Kikuchi, Okabe and Fujio [16] in 1999, Zhang and Kikuchi [35] in 2000, Arnold, Boffi and Falk [3] in 2002, Rajendran and Liew [28] in 2003, Li et al. [19] in 2004, Cen and coauthors [12] in 2010, Arnold and Awanou [2] in 2011, and Rand, Gillette and Bajaj [29] in 2014, and so on.

Compared with the FEM, the finite volume method (FVM) ensures the local conservation law, which makes it widely used in scientific and engineering computations, see [4, 18, 27, 31] for an incomplete references. The finite volume element method (FVEM) is a member of FVM. The mathematical development of linear FVEM on triangular mesh is almost as satisfactory as linear FEM, see [20, 22, 36] and the references cited therein. For the bilinear FVE scheme on quadrilateral mesh, most existing works need the quasi-parallel quadrilateral assumption (e.g., [21, 23, 24, 37]), and recently [14] present a sufficient condition which covers the traditional $h^{1+\gamma}$-parallelogram mesh condition to guarantee the coercivity result.

However, it is still a challenging task to construct and analyze high order FVE schemes with optimal convergence orders, e.g., [8, 9, 20, 23, 25, 32–34, 37]. In particular, for the second order scheme, under the $h^{1+\gamma}$-parallelogram mesh assumption, [23, 37] bring the uniform stability and optimal convergence rates under both H^1 and L^2 norms. On the triangular meshes, the unconditionally stable quadratic scheme in [42] does not guarantee the optimal convergence rate in L^2 norm. Under the minimum angle condition 1.42° [39, 40], the second order scheme in [32]

Received by the editors October 28, 2019 and, in revised form, November 19, 2020.
2000 *Mathematics Subject Classification.* 35R35, 49J40, 60G40.

owns the optimal L^2 norm error estimate. Recently, [38] presents a class of bubble enriched quadratic schemes such that the convergence order of L^2 error is 3, regrettably the unconditionally stable of these schemes are not proved. In summary, the construction and analysis of second order FVE schemes are not easy, and the research of serendipity FVE scheme is little.

In this paper, we study the serendipity finite element method in a way different from the aforementioned works. Precisely, we post-process the eight-nodes-serendipity finite element solution so that it satisfies a desired property–the conservation law in element level. For this purpose, we first enlarge the classic serendipity finite element space by adding eight bubbles on each element. Then we construct the associated *control volumes*, each of which is a polygon surrounding a *node* of the mesh constructed by dividing each parallelepiped element with two special points on each edge and five special points (whose locations depend on the same single parameter) in the interior of the element. At the end, by solving an 8-by-8 linear system on each element, we devise our post-processed solution such that the conservation law holds on each *control volume*. Since the bubbles are the polynomials in the interior of each element and vanish at the edge of the element, the post-processed solution is globally continuous in the whole domain. More importantly, not only the post-processed solution guarantees the element-level conservation law, but also makes sure of the optimal convergence rates under both H^1 and L^2 norms.

In comparison with the FVEM, we demonstrate the importance of our results in what follows. Through comparing with the second order scheme in [37], we can see clearly that : 1) the linear system derived from the eight nodes serendipity element is symmetric, while that derived from the second order scheme in [37] is unsymmetric; 2) under the same mesh, the degree of the freedoms of the eight nodes serendipity element is much less than that of the scheme in [37]; 3) our post-processing procedure is performed on each element independently, and thus can be implemented in a parallel computing environment. In summary, directing at the high computing cost and the difficulties resided in devising and analyzing the high order FVEMs, the techniques presented here supply a better option for producing the local conservative solution and owning the optimal convergence rates. Note that the relevant works on the postprocessing technique for Lagrange finite element solution can be found in [7, 13, 43] and the references cited therein.

The rest of this paper is organized as follows. In the next section we introduce the serendipity finite elements and associated control volumes. In Section 3 we postprocess the serendipity finite element solution such that it satisfies the local conservation law on each control volume. The property that the post-processed solution owns the optimal convergence rate will be rigourously proved in this section. Numerical examples are presented in Section 4 to validate our theoretical findings. Some concluding remarks are given in Section 5.

To avoid repetition, we write "$A \lesssim B$" meaning that A can be bounded by B with a constant multiple irrelative to the parameters which A and B may depend on, while "$A \gtrsim B$" meaning that B can be bounded by A. "$A \sim B$" indicates that "$A \lesssim B$" as well as "$B \lesssim A$".

2. The serendipity finite elements and associated control volumes

We consider the finite element method for the elliptic model problem :

$$-\nabla \cdot (\beta \nabla u) = f \quad \text{in } \Omega, \tag{1}$$

$$u = 0 \quad \text{on } \partial\Omega, \tag{2}$$

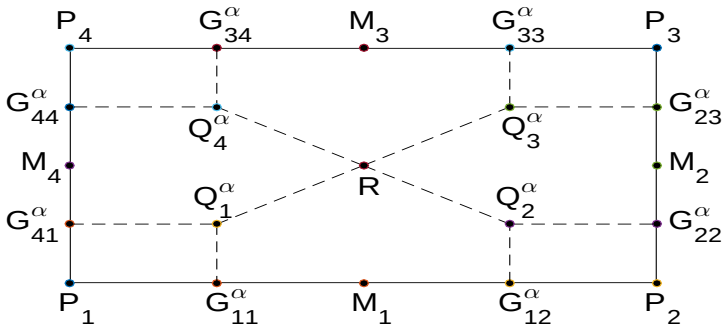

FIGURE 1. Partition (dotted lines) of the rectangular element $P_1P_2P_3P_4$.

where $\Omega = [a,b]\times[c,d]$ is a rectangle, $f \in L^2(\Omega)$, and there exist positive constants $\beta_{\min}$, $\beta_{\max}$ such that for all $(x_1,x_2)\in\Omega$

$$0 < \beta_{\min} \le \beta(x_1,x_2) \le \beta_{\max} < +\infty.$$

Let $\mathcal{T}_h$ be a *conform* and *shape regular* rectangular mesh of Ω, with mesh size h, we define the finite element space

$$U_h = \{v \in C(\overline{\Omega}) :\ v|_\tau \in Q_2^*,\ \forall\,\tau\in\mathcal{T}_h;\ v|_{\partial\Omega} = 0\},$$

where

$$Q_2^* := \mathrm{Span}\{1, x_1, x_2, x_1x_2, x_1^2, x_2^2, x_1^2x_2, x_1x_2^2\}$$

is the 2nd order serendipity set of polynomials. The serendipity finite element solution for (1) and (2) is the function $u_h \in U_h$ satisfying

$$a(u_h, v_h) = (f, v_h), \quad \forall\, v_h \in U_h, \tag{3}$$

with the bilinear form

$$a(v,w) = \int_\Omega \beta\nabla v\cdot\nabla w\,\mathrm{d}x_1\mathrm{d}x_2, \quad \forall\, v,w\in H^1(\Omega),$$

and the right-hand side $(f,v_h) = \int_\Omega f v_h\,\mathrm{d}x_1\mathrm{d}x_2$. If $u\in H^3(\Omega)$, it is known that there hold the following error estimates (c.f. [5,6,10])

$$\|u-u_h\|_m \lesssim h^{3-m}\|u\|_3, \quad m = 0,1.$$

Next we introduce the *control volumes* associated with $\mathcal{T}_h$. For each rectangle $\tau = \square P_1P_2P_3P_4 \in \mathcal{T}_h$, let M_i, $i\in\mathbb{Z}_4$ be the midpoint of the line segment P_iP_{i+1} (see Figure 1), and let R be the intersection of P_1P_3 and P_2P_4, where $\mathbb{Z}_n = \{1,2,\cdots,n\}$, $P_5 := P_1$. Given $\alpha\in(0,1)$ and $i\in\mathbb{Z}_4$, let $G_{i,i}^\alpha$ and $G_{i,i+1}^\alpha$ be the points on P_iP_{i+1} satisfying

$$\frac{|M_iG_{i,i}^\alpha|}{|M_iP_i|} = \frac{|M_iG_{i,i+1}^\alpha|}{|M_iP_{i+1}|} = \alpha,$$

where $G_{4,5}^\alpha := G_{4,1}^\alpha$, and let the points $Q_i^\alpha \in \overline{RP_i}$ satisfying

$$\frac{|RQ_i^\alpha|}{|RP_i|} = \alpha.$$

Moreover, we denote by $\mathcal{N}_h^\tau = \{P_1,P_2,P_3,P_4,M_1,M_2,M_3,M_4\}$ the set of 8 nodes on τ. Let $\mathcal{N}_h = \bigcup_{\tau\in\mathcal{T}_h}\mathcal{N}_h^\tau$ be the set of all nodes of $\mathcal{T}_h$ and $\mathcal{N}_h^\circ = \mathcal{N}_h\backslash\partial\Omega$ the set

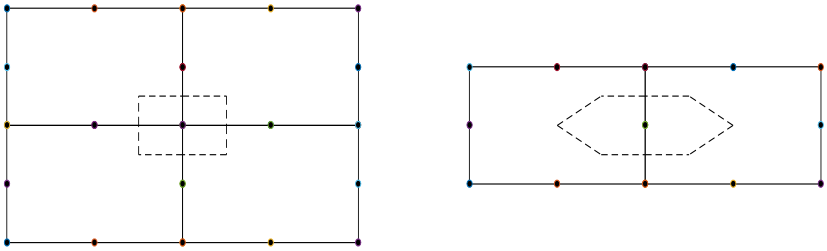

FIGURE 2. Control volumes with respect to a vertex (left) and a midpoint (right).

of all interior nodes of $\mathcal{T}_h$. For all $P \in \mathcal{N}_h$, we denote the patch $w_P = \cup\{\tau \in \mathcal{T}_h : \overline{\tau} \ni P\}$, where $\overline{\tau} := \tau \cup \partial\tau$. For each $\tau \in \mathcal{T}_h$, let $w_\tau = \cup\{\tau_1 \in \mathcal{T}_h : \overline{\tau} \cap \overline{\tau}_1 \neq \emptyset\}$.

We are now ready to define the control volume for each node $P \in \mathcal{N}_h$. If P is a vertex of τ, $P = P_i$ in the element τ, then we let the contribution from τ to control volume V_{P_i} is the rectangle $V_{\tau,P_i} := P_i G^\alpha_{i,i} Q^\alpha_i G^\alpha_{i-1,i}$ with $G^\alpha_{01} = G^\alpha_{41}$, $i \in \mathbb{Z}_4$. If P is a midpoint of the edge of τ, $P = M_i$, then the contribution from τ to the control volume V_{M_i} is the polygon $V_{\tau,M_i} := G^\alpha_{i,i} G^\alpha_{i,i+1} Q^\alpha_{i+1} R Q^\alpha_i$ with $Q^\alpha_5 = Q^\alpha_1$, $i \in \mathbb{Z}_4$. For all $P \in \mathcal{N}_h$, the whole control volume surrounding point P is defined as

$$V_P = \bigcup_{\overline{\tau} \ni P} V_{\tau,P},$$

see Figure 2 for the control volume associated with a vertex P and/or with a midpoint M.

All control volumes V_P constitute a so-called *dual mesh* $\mathcal{T}'_h = \{V_P : P \in \mathcal{N}_h\}$. The test function space V_h with respect to $\mathcal{T}'_h$ is defined as

$$V_h = \mathrm{Span}\{\psi_{V_P} : P \in \mathcal{N}_h^\circ\},$$

where ψ_{V_P} is the characteristic function on V_P. From the finite element space U_h to the test function space V_h, we define a mapping Π as

$$v_h^* := \Pi v_h = \sum_{P \in \mathcal{N}_h^\circ} v_h(P)\psi_{V_P} \in V_h, \quad \forall\, v_h \in U_h.$$

3. Postprocessing

Generally speaking, the serendipity finite element solution u_h does not satisfy the following local conservation law

$$\int_{V_P} f \,\mathrm{d}x_1\mathrm{d}x_2 + \int_{\partial V_P} \beta \frac{\partial u_h}{\partial \boldsymbol{n}} \,\mathrm{d}s = 0,$$

on each control volume V_P, $P \in \mathcal{N}_h^\circ$, where $\boldsymbol{n}$ is the unit outward normal on the boundary ∂V_P. In this section, we postprocess the serendipity finite element solution u_h of (3) to generate a continuous function $\hat{u}_h$ which satisfies the local conservation law on each control volume V_P, $P \in \mathcal{N}_h^\circ$.

To this end, we first introduce the *bubbles* on each rectangular element $\tau = \square P_1P_2P_3P_4$. Let φ_j, $j \in \mathbb{Z}_4$ be the four bilinear basis functions associated with the

four vertices P_i, $i \in \mathbb{Z}_4$ of τ satisfying

$$\varphi_j(P_i) = \delta_{ij}, \quad i, j \in \mathbb{Z}_4,$$

and ϕ_j, $j \in \mathbb{Z}_8$ be the eight serendipity basis functions associated with the four vertices P_i, $i \in \mathbb{Z}_4$ and four midpoints M_i, $i \in \mathbb{Z}_4$ of τ satisfying

$$\phi_j(P_i) = \delta_{ij}, \quad i, j \in \mathbb{Z}_8,$$

where $\delta_{ij} = 1$ if $i = j$, $\delta_{ij} = 0$ if $i \neq j$, and $P_{i+4} := M_i$, $i \in \mathbb{Z}_4$. We denote by $r = |P_1P_2|/|P_1P_4|$ the ratio between the length and height of τ, and introduce two polynomials

$$p(r) = -4500r^6 + 79427r^4 + 100219r^2 + 16292,$$
$$q(r) = 17025140r^8 + 49059091r^6 - 186752204r^4 + 98377715r^2 - 4702500.$$

It is easy to obtain that the three positive roots of q are

$$r_1 = \sqrt{\frac{\sqrt{7336997329} - 83927}{32584}},\ r_2 = \sqrt{\frac{1186 - \sqrt{314571}}{1045}},\ r_3 = \sqrt{\frac{1186 + \sqrt{314571}}{1045}},$$

and the positive root of p is

$$r_4 = \sqrt{\frac{\sqrt{7336997329} + 83927}{9000}}.$$

Obviously, we have $r_1r_4 = r_2r_3 = 1$. If $|r - r_i| > \varepsilon_0 = 10^{-3}$, $\forall\, i \in \mathbb{Z}_4$, we define the bubbles on τ by

$$\begin{aligned} \psi_j = \psi_j^\tau &= \varphi_1\varphi_3\varphi_j, \quad j \in \mathbb{Z}_4, \\ \psi_j = \psi_j^\tau &= \varphi_1\varphi_3\phi_j, \quad j \in \mathbb{Z}_8\backslash\mathbb{Z}_4. \end{aligned} \tag{4}$$

If $|r - r_i| \leq \varepsilon_0$ for some $i \in \mathbb{Z}_4$, we define the bubbles as

$$\begin{aligned} \psi_j = \psi_j^\tau &= \varphi_1\varphi_3\varphi_j, \quad j \in \{2, 4\}, \\ \psi_j = \psi_j^\tau &= \varphi_1\varphi_3\phi_j, \quad j \in \mathbb{Z}_8\backslash\{2, 4\}. \end{aligned} \tag{5}$$

We define the enlarged function space

$$\widehat{U}_h = U_h \oplus \mathrm{Span}\{\psi_j^\tau : \tau \in \mathcal{T}_h,\ j \in \mathbb{Z}_8\}.$$

Since ψ_j^τ, $j \in \mathbb{Z}_8$ vanish on the boundary of τ, each function $\widehat{u}_h \in \widehat{U}_h$ is still continuous in the whole Ω.

Next we introduce a functional $R(\cdot, \cdot, \cdot)$ defined for all $w_h \in U_h$ and all $\tau \in \mathcal{T}_h$ by

$$\begin{aligned} &R(f, w_h, \tau) \\ &= \int_\tau f(w_h^* - w_h)\,\mathrm{d}x_1\mathrm{d}x_2 + \int_\tau \beta\nabla u_h \cdot \nabla w_h\,\mathrm{d}x_1\mathrm{d}x_2 + \int_{\partial\tau} \{\beta\nabla u_h\} \cdot \boldsymbol{n}(w_h^* - w_h)\,\mathrm{d}s, \end{aligned}$$

where $\{\cdot\}$ is an averaging operator which defined on $\partial\tau$, i.e., if τ_1 and τ_2 are two neighbour elements, the edge $E = \overline{\tau}_1 \cap \overline{\tau}_2$, then for all vectorial function $\boldsymbol{v}$ which has been well defined in the interior of τ_1 and τ_2,

$$\{\boldsymbol{v}\}_E = \frac{1}{2}\left(\boldsymbol{v}|_{E,\overline{\tau}_1} + \boldsymbol{v}|_{E,\overline{\tau}_2}\right).$$

Now on each $\tau \in \mathcal{T}_h$, let

$$\widehat{u}_h = u_h + \sum_{j=1}^{8} c_j\psi_j \in \widehat{U}_h, \tag{6}$$

satisfies the constraints

$$-\int_{(\partial V_{P_i})\cap\tau}\beta\frac{\partial\widehat{u}_h}{\partial\boldsymbol{n}}\,\mathrm{d}s=R(f,\phi_{P_i},\tau),\quad i\in\mathbb{Z}_8 \tag{7}$$

and the constraint

$$\widehat{u}_h(O)=u_h(O), \tag{8}$$

where $O:=O_\tau$ is the barycenter of the element τ.

Assume the parameter $\alpha=1/2$, the bubbles are defined in (4) and (5), and $\widehat{u}_h$ is constructed by (6), then there exists one unique $\widehat{u}_h$ such that (7) and (8) hold, see Theorem 3.1. Moreover, for any $\alpha\in(0,1)$, the postprocessed solution $\widehat{u}_h$ satisfies the local conservation law, and converges to the exact solution with optimal convergence orders under both H^1 and L^2 error norms, see Theorem 3.2.

Theorem 3.1. *Suppose the coefficient β is piecewise constant with respect to $\mathcal{T}_h$, or piecewise $W^{1,\infty}$ and the mesh size h is sufficiently small, the parameter $\alpha=1/2$. Then for each $\tau\in\mathcal{T}_h$, there exists one unique $\widehat{u}_h$ which satisfies* (7) *and* (8) *simultaneously.*

Proof. We first prove the theorem for the case that β is a constant in τ. For each $\tau\in\mathcal{T}_h$, by (6) and (7), there holds

$$-\int_{(\partial V_{P_i})\cap\tau}\beta\nabla\left(\sum_{j=1}^{8}c_j\psi_j\right)\cdot\boldsymbol{n}\,\mathrm{d}s=-\int_{(\partial V_{P_i})\cap\tau}\beta\nabla(\widehat{u}_h-u_h)\cdot\boldsymbol{n}\,\mathrm{d}s=RHS_i,\ i\in\mathbb{Z}_8,$$

where

$$RHS_i=R(f,\phi_{P_i},\tau)+\int_{(\partial V_{P_i})\cap\tau}\beta\nabla u_h\cdot\boldsymbol{n}\,\mathrm{d}s.$$

This leads to the linear algebraic system

$$\widetilde{A}\mathbf{c}=\widetilde{\mathbf{b}}, \tag{9}$$

where $\mathbf{c}=(c_i)_{8\times1}$ is the unknown vector, $\widetilde{A}=(\widetilde{a}_{ij})_{8\times8}$ with the entries

$$\widetilde{a}_{ij}=-\int_{(\partial V_{P_i})\cap\tau}\beta\nabla\psi_j\cdot\boldsymbol{n}\,\mathrm{d}s,\quad i,j\in\mathbb{Z}_8$$

and $\widetilde{\mathbf{b}}=(\widetilde{b}_i)_{8\times1}$ with the entries

$$\widetilde{b}_i=RHS_i,\quad i\in\mathbb{Z}_8.$$

Observing that ψ_j and u_h are continuous in τ, we have that

$$\sum_{i=1}^{8}\int_{(\partial V_{P_i})\cap\tau}\beta\nabla\psi_j\cdot\boldsymbol{n}\,\mathrm{d}s=\sum_{i=1}^{8}\int_{(\partial V_{P_i})\cap\tau}\beta\nabla u_h\cdot\boldsymbol{n}\,\mathrm{d}s=0,\quad j\in\mathbb{Z}_8.$$

Therefore, we obtain

$$\sum_{i=1}^{8}\widetilde{a}_{ij}=0,\quad\forall\, j\in\mathbb{Z}_8$$

and

$$\begin{aligned}\sum_{i=1}^{8}RHS_i&=\sum_{i=1}^{8}\left(R(f,\phi_{P_i},\tau)+\int_{(\partial V_{P_i})\cap\tau}\beta\nabla u_h\cdot\boldsymbol{n}\,\mathrm{d}s\right)\\&=R\left(f,\sum_{i=1}^{8}\phi_{P_i},\tau\right)=R(f,1,\tau)=0,\end{aligned}$$

which implies the system of equations (9) are linear dependent.

We now replace the last equation of (9) by (8) and then multiply both sides of the novel eight equations by 64 to obtain a novel system

$$A\mathbf{c} = \mathbf{b}. \tag{10}$$

To show the existence and uniqueness of $\widehat{u}_h$, we only need to show that A is a nonsingular matrix. In the following, we verify the nonsingular property of A for the case that $|r - r_i| > \varepsilon_0 = 10^{-3}$, $\forall\, i \in \mathbb{Z}_4$. In this case, by direct calculations, we obtain

$$a_{8j} = 1,\ a_{8,j+4} = 2, \quad j \in \mathbb{Z}_4,$$

and

$$a_{11} = -\frac{67}{256}\beta\left(r + \frac{1}{r}\right),\quad a_{21} = -\beta\left(\frac{13r}{256} + \frac{335}{768r}\right),\quad a_{31} = -\frac{65}{768}\beta\left(r + \frac{1}{r}\right),$$
$$a_{41} = -\beta\left(\frac{335r}{768} + \frac{13}{256r}\right),\quad a_{51} = \beta\left(\frac{4r}{15} + \frac{613}{480r}\right),\quad a_{61} = \beta\left(\frac{69r}{160} - \frac{137}{120r}\right),$$
$$a_{71} = \beta\left(\frac{69}{160r} - \frac{137r}{120}\right),\quad a_{62} = \beta\left(\frac{613r}{480} + \frac{4}{15r}\right),\quad a_{15} = -\beta\left(\frac{53r}{320} + \frac{67}{64r}\right),$$
$$a_{35} = -\beta\left(\frac{53r}{192} + \frac{13}{64r}\right),\quad a_{55} = \beta\left(\frac{1873r}{3360} + \frac{13843}{3360r}\right),\quad a_{65} = \beta\left(\frac{97r}{80} - \frac{37}{24r}\right),$$
$$a_{75} = \beta\left(\frac{1639}{1120r} - \frac{2351r}{1120}\right),\quad a_{16} = -\beta\left(\frac{13r}{64} + \frac{53}{192r}\right),\ a_{26} = -\beta\left(\frac{67r}{64} + \frac{53}{320r}\right),$$
$$a_{56} = \beta\left(\frac{97}{80r} - \frac{37r}{24}\right),\quad a_{66} = \beta\left(\frac{13843r}{3360} + \frac{1873}{3360r}\right),\ a_{68} = \beta\left(\frac{1639r}{1120} - \frac{2351}{1120r}\right)$$

and

$$\begin{aligned}
&a_{12} = a_{21}, \quad a_{22} = a_{11}, \quad a_{32} = a_{41}, \quad a_{42} = a_{31}, \quad a_{52} = a_{51}, \quad a_{72} = a_{71},\\
&a_{13} = a_{31}, \quad a_{23} = a_{41}, \quad a_{33} = a_{11}, \quad a_{43} = a_{21}, \quad a_{53} = a_{71}, \quad a_{63} = a_{62},\\
&a_{73} = a_{51}, \quad a_{14} = a_{32}, \quad a_{24} = a_{42}, \quad a_{34} = a_{12}, \quad a_{44} = a_{22}, \quad a_{54} = a_{72},\\
&a_{64} = a_{61}, \quad a_{74} = a_{52}, \quad a_{25} = a_{15}, \quad a_{45} = a_{35}, \quad a_{36} = a_{26}, \quad a_{46} = a_{16},\\
&a_{76} = a_{56}, \quad a_{17} = a_{35}, \quad a_{27} = a_{45}, \quad a_{37} = a_{15}, \quad a_{47} = a_{25}, \quad a_{57} = a_{75},\\
&a_{67} = a_{65}, \quad a_{77} = a_{55}, \quad a_{18} = a_{36}, \quad a_{28} = a_{46}, \quad a_{38} = a_{16}, \quad a_{48} = a_{26},\\
&a_{58} = a_{76}, \quad a_{78} = a_{56}.
\end{aligned}$$

Using the software *Matlab*, we get

$$\det(A) = -\frac{\beta^7 p(r) q(r)}{38535168000000 r^7}.$$

Since the ratio r satisfies the conditions $|r - r_i| > \varepsilon_0 = 10^{-3}$, $\forall\, i \in \mathbb{Z}_4$, we have $\det(A) \neq 0$ and thus the system (10) has a unique solution. Namely, there exists a unique $\widehat{u}_h$ which satisfies (7) and (8) simultaneously. The proof for the case that $|r - r_i| \leq \varepsilon_0$ for some $i \in \mathbb{Z}_4$ is similar and thus we omit it here.

Next we consider the general case that β is piecewise $W^{1,\infty}$ with respect to $\mathcal{T}_h$. We denote

$$\overline{\beta}\big|_\tau = \frac{1}{|\tau|}\int_\tau \beta \,\mathrm{d}x_1\mathrm{d}x_2, \quad \forall\, \tau \in \mathcal{T}_h,$$

where $|\tau|$ is the area of τ. Consequently, $\overline{\beta}$ is piecewise constant, $\beta_{\min} \leq \overline{\beta} \leq \beta_{\max}$ and $\|\beta - \overline{\beta}\|_{0,\infty,\tau} \lesssim h$. Then we can define a matrix $\overline{A} = (\overline{a}_{ij})_{8\times 8}$ corresponding to

$\overline{\beta}$ as above. From the above reasoning, we have

$$\det(\overline{A}) \sim 1.$$

On the other hand, the fact that $|a_{ij} - \overline{a}_{ij}| \lesssim h$, $i, j \in \mathbb{Z}_8$ yields that

$$|\det(A) - \det(\overline{A})| \lesssim h.$$

Therefore, when h is sufficiently small, we get $\det(A) \neq 0$, and there exists a unique $\widehat{u}_h$ satisfying (7) and (8) simultaneously. The proof is complete. □

Remark 3.1. *If $\alpha \neq 1/2$, one may choose other appropriate bubble functions to ensure the existence and uniqueness of $\widehat{u}_h$ which satisfies* (7) *and* (8) *simultaneously.*

Theorem 3.2. *The postprocessed solution $\widehat{u}_h$ satisfies the local conservation property*

$$-\int_{\partial V_P} \beta \frac{\partial \widehat{u}_h}{\partial \boldsymbol{n}} \,\mathrm{d}s = \int_{V_P} f \,\mathrm{d}x_1\mathrm{d}x_2 \tag{11}$$

on each control volume V_P, $\forall P \in \mathcal{N}_h^\circ$. Moreover, we have the optimal-order L^2 and H^1 error estimates

$$\|u - \widehat{u}_h\|_m \lesssim h^{3-m}\|u\|_3, \quad m = 0, 1. \tag{12}$$

Proof. We observe that for all $P \in \mathcal{N}_h^\circ$,

$$\phi_P^*|_{\partial w_P} = \phi_P|_{\partial w_P} = 0,$$

and for all $\tau \in w_P$, the jump

$$[\{\beta \nabla u_h\} \cdot \boldsymbol{n}]_{(\partial\tau)\backslash(\partial w_P)} = 0.$$

Therefore

$$\sum_{\tau \in w_P} \int_{\partial\tau} \{\beta \nabla u_h\} \cdot \boldsymbol{n} \phi_P^* \,\mathrm{d}s = \sum_{\tau \in w_P} \int_{\partial\tau} \{\beta \nabla u_h\} \cdot \boldsymbol{n} \phi_P \,\mathrm{d}s = 0.$$

Then by (7), we have

$$\begin{aligned}
-\int_{\partial V_P} \beta \frac{\partial \widehat{u}_h}{\partial \boldsymbol{n}} \,\mathrm{d}s &= -\sum_{\tau \in w_P} \int_{(\partial V_P)\cap\tau} \beta \frac{\partial \widehat{u}_h}{\partial \boldsymbol{n}} \,\mathrm{d}s \\
&= \sum_{\tau \in w_P} R(f, \phi_P, \tau) \\
&= \sum_{\tau \in w_P} \left(\int_\tau f(\phi_P^* - \phi_P) \,\mathrm{d}x_1\mathrm{d}x_2 + \int_\tau \beta \nabla u_h \cdot \nabla \phi_P \,\mathrm{d}x_1\mathrm{d}x_2 \right) \\
&= \int_\Omega f(\phi_P^* - \phi_P) \,\mathrm{d}x_1\mathrm{d}x_2 + \int_\Omega \beta \nabla u_h \cdot \nabla \phi_P \,\mathrm{d}x_1\mathrm{d}x_2 \\
&= \int_{V_P} f \,\mathrm{d}x_1\mathrm{d}x_2,
\end{aligned}$$

where we have used the facts that $\phi_P^* = 1$ in V_P and $\phi_P^* = 0$ in $\Omega\backslash V_P$. The local conservation property (11) is verified.

To prove (12), we only need to estimate $\widehat{u}_h - u_h = \sum_{j=1}^8 c_j \psi_j$ in each τ. Note that c_j, $j \in \mathbb{Z}_8$ satisfies $A\mathbf{c} = \mathbf{b}$. Moreover, by Theorem 3.1, there hold $|a_{ij}| \lesssim 1$, $i, j \in \mathbb{Z}_8$ and $\det(A) \sim 1$. Then $\|A^{-1}\|_\infty \lesssim 1$ and we obtain

$$|c_j| \lesssim \max_{1 \le i \le 8} |RHS_i|, \quad \forall\, j \in \mathbb{Z}_8.$$

Next we estimate RHS_i. It follows from the Green's formula that

$$\begin{aligned}\int_\tau f\phi^*_{P_i}\,\mathrm{d}x_1\mathrm{d}x_2 &= \int_{V_{P_i}\cap\tau} f\,\mathrm{d}x_1\mathrm{d}x_2 = -\int_{V_{P_i}\cap\tau}\nabla\cdot(\beta\nabla u)\,\mathrm{d}x_1\mathrm{d}x_2\\ &= -\int_{\partial(V_{P_i}\cap\tau)}\beta\nabla u\cdot\boldsymbol{n}\,\mathrm{d}s\end{aligned}$$

and

$$\begin{aligned}\int_\tau f\phi_{P_i}\,\mathrm{d}x_1\mathrm{d}x_2 &= -\int_\tau\nabla\cdot(\beta\nabla u)\phi_{P_i}\,\mathrm{d}x_1\mathrm{d}x_2\\ &= \int_\tau\beta\nabla u\cdot\nabla\phi_{P_i}\,\mathrm{d}x_1\mathrm{d}x_2 - \int_{\partial\tau}\beta\nabla u\cdot\boldsymbol{n}\phi_{P_i}\,\mathrm{d}s.\end{aligned}$$

Then

$$\begin{aligned}RHS_i &= R(f,\phi_{P_i},\tau) + \int_{(\partial V_{P_i})\cap\tau}\beta\nabla u_h\cdot\boldsymbol{n}\,\mathrm{d}s\\ &= \int_\tau f(\phi^*_{P_i}-\phi_{P_i})\,\mathrm{d}x_1\mathrm{d}x_2 + \int_\tau\beta\nabla u_h\cdot\nabla\phi_{P_i}\,\mathrm{d}x_1\mathrm{d}x_2\\ &\quad + \int_{\partial\tau}\{\beta\nabla u_h\}\cdot\boldsymbol{n}(\phi^*_{P_i}-\phi_{P_i})\,\mathrm{d}s + \int_{(\partial V_{P_i})\cap\tau}\beta\nabla u_h\cdot\boldsymbol{n}\,\mathrm{d}s\\ &= \int_\tau\beta\nabla(u_h-u)\cdot\nabla\phi_{P_i}\,\mathrm{d}x_1\mathrm{d}x_2 + \int_{(\partial V_{P_i})\cap\tau}\beta\nabla(u_h-u)\cdot\boldsymbol{n}\,\mathrm{d}s\\ &\quad + \int_{V_{P_i}\cap\partial\tau}(\{\beta\nabla u_h\}-\beta\nabla u)\cdot\boldsymbol{n}\,\mathrm{d}s + \int_{\partial\tau}(\beta\nabla u-\{\beta\nabla u_h\})\cdot\boldsymbol{n}\phi_{P_i}\,\mathrm{d}s\\ &\triangleq I_1+I_2+I_3+I_4.\end{aligned}$$

It is easy to verify that

$$|I_1|\lesssim|u-u_h|_{1,\tau}$$

and

$$\begin{aligned}|I_2| &\lesssim h_\tau^{\frac{1}{2}}\left|\int_{(\partial V_{P_i})\cap\tau}|\nabla(u_h-u)|^2\,\mathrm{d}s\right|^{\frac{1}{2}}\\ &\lesssim|u-u_h|_{1,\tau}+h_\tau|u-u_h|_{2,\tau},\end{aligned}$$

where h_τ is the diameter of τ. On the other hand

$$\begin{aligned}|I_3|+|I_4| &\lesssim \int_{\partial\tau}|\{\beta\nabla u_h\}-\beta\nabla u|\,\mathrm{d}s\\ &\lesssim h_\tau^{\frac{1}{2}}\left|\int_{\partial\tau}|\{\beta\nabla u_h\}-\beta\nabla u|^2\,\mathrm{d}s\right|^{\frac{1}{2}}\\ &\lesssim|u-u_h|_{1,w_\tau}+h_\tau|u-u_h|_{2,w_\tau}.\end{aligned}$$

Combining the above inequalities

$$|RHS_i|\lesssim|u-u_h|_{1,w_\tau}+h_\tau|u-u_h|_{2,w_\tau},\quad\forall\, i\in\mathbb{Z}_8.$$

Note that

$$\begin{aligned}|u-u_h|_{2,\tau} &\le |u-u_I|_{2,\tau}+|u_I-u_h|_{2,\tau}\\ &\lesssim h_\tau\|u\|_{3,\tau}+h_\tau^{-1}\|u_I-u_h\|_{1,\tau}\\ &\lesssim h_\tau\|u\|_{3,\tau}+h_\tau^{-1}(\|u-u_I\|_{1,\tau}+\|u-u_h\|_{1,\tau})\\ &\lesssim h_\tau\|u\|_{3,\tau}+h_\tau^{-1}\|u-u_h\|_{1,\tau},\end{aligned}$$

where $u_I \in U_h$ is the piecewise interpolation such that for each rectangular element $\tau = \Box P_1P_2P_3P_4$

$$u_I(P_i) = u(P_i),\ u_I(M_i) = u(M_i), \quad i \in \mathbb{Z}_4.$$

Thus, for $m = 0, 1$

$$\begin{aligned}
\|\widehat{u}_h - u_h\|_{m,\tau} &= \left\| \sum_{j=1}^{8} c_j \psi_j \right\|_{m,\tau} \\
&\leq \sum_{j=1}^{8} |c_j| \|\psi_j\|_{m,\tau} \\
&\lesssim h_\tau^{1-m} \max_{1\leq j\leq 8} |c_j| \\
&\lesssim h_\tau^{1-m} \max_{1\leq i\leq 8} |RHS_i| \\
&\lesssim h_\tau^{1-m} |u - u_h|_{1,w_\tau} + h_\tau^{3-m} \|u\|_{3,w_\tau}.
\end{aligned}$$

Summing up the above inequality over all elements, we obtain

$$\|\widehat{u}_h - u_h\|_m \lesssim h^{3-m} \|u\|_3.$$

Finally, by the triangle inequality

$$\|u - \widehat{u}_h\|_m \leq \|u - u_h\|_m + \|u_h - \widehat{u}_h\|_m,$$

we get the desired estimates (12). □

Remark 3.2. *For the L^2 error estimate of second order FVE schemes, the regularity assumptions in [23, 38] are $(u, f) \in H^3 \times H^2$, and the regularity assumption in [32] is $u \in H^4$. In this paper, the assumption is $u \in H^3$, lower than [23, 32, 38]. Moreover, the stiffness matrix generated from finite element scheme is symmetric and positive definite which more easier to solve.*

4. Numerical examples

In this section, we present three numerical examples to validate our postprocessing technique. Examples 4.1 and 4.2 are designed for elliptic and parabolic equation respectively, while Example 4.3 is for a single phase flow model. In these examples, we choose $\Omega = [0, 1]^2$ and the rectangular meshes $\mathcal{T}_k = \mathcal{T}_{h_k}$, $k \in \mathbb{Z}_7$, are obtained by uniformly refining the rectangle $[0, 1]^2$, where $h_k = 2^{-k}$ is the mesh size of $\mathcal{T}_k$.

Example 4.1. We consider the problem (1), (2) with the discontinuous coefficient

$$\beta(x_1, x_2) = \begin{cases} 1, & x_1 \leq 0.5, \\ 2, & x_1 > 0.5, \end{cases}$$

and the discontinuous right-hand-side function

$$f(x_1, x_2) = \begin{cases} -8x_1e^{2x_2} - 2, & x_1 \leq 0.5, \\ -8x_1e^{2x_2} - 4e^{2x_2} - 4, & x_1 > 0.5. \end{cases}$$

The problem has the exact solution

$$u(x_1, x_2) = \begin{cases} 2x_1e^{2x_2} + x_2^2, & x_1 \leq 0.5, \\ x_1e^{2x_2} + 0.5e^{2x_2} + x_2^2, & x_1 > 0.5. \end{cases}$$

In our numerical experiment, we first use (3) to compute the serendipity finite element solution u_h. Then we postprocess u_h on three kinds of control volumes: $\alpha = 1/3,\ 2/5,\ 1/2$, and use $\widehat{u}_h$ to denote the post-processed solution which satisfies

TABLE 1. Postprocess errors and convergence orders for Example 4.1, $\alpha = 1/3$.

h	$\lvert LCE(u_h)\rvert_S$	Order	$\lvert LCE(\widehat{u}_h)\rvert_M$	$\lvert u-\widehat{u}_h\rvert_1$	Order	$\lVert u-\widehat{u}_h\rVert_0$	Order
1/2	2.09e-01	/	2.48e-14	4.04e-01	/	1.80e-02	/
1/4	9.31e-02	1.166	3.57e-14	9.55e-02	2.081	1.79e-03	3.330
1/8	2.96e-02	1.652	4.97e-14	2.28e-02	2.069	1.79e-04	3.315
1/16	8.29e-03	1.837	5.53e-14	5.58e-03	2.028	2.01e-05	3.157
1/32	2.19e-03	1.921	5.18e-14	1.39e-03	2.009	2.42e-06	3.054
1/64	5.62e-04	1.961	5.73e-14	3.46e-04	2.002	2.99e-07	3.016
1/128	1.43e-04	1.981	6.18e-14	8.65e-05	2.001	3.73e-08	3.004

(7) and (8). Noticing that the ratio $r = 1$ for each rectangular element $\tau \in \mathcal{T}_k$, thus we choose the bubbles defined in (4).

In order to compare the local-conservation-errors (LCEs) of finite element solution and its postprocessed finite-volume-element-like solution, we define the LCE associated with a control volume V_P as

$$LCE_P(v_h) = \int_{V_P} f \,\mathrm{d}x_1\mathrm{d}x_2 + \int_{\partial V_P} \beta \frac{\partial v_h}{\partial \boldsymbol{n}} \,\mathrm{d}s, \quad \forall\, v_h \in H^1(\Omega).$$

Moreover, we denote

$$|LCE(v_h)|_S = \sum_{P\in\mathcal{N}_h^\circ} |LCE_P(v_h)| \quad \text{and} \quad |LCE(v_h)|_M = \max_{P\in\mathcal{N}_h^\circ} |LCE_P(v_h)|$$

as the summation and maximum of these errors respectively.

The numerical results are reported in Tables 1-3 and "Order" indicates the numerical convergence order computed by $\log_2(E_{2h}/E_h)$, where E_{2h} and E_h are the errors of the corresponding two successive mesh size $\mathcal{T}_{2h}$ and $\mathcal{T}_h$. We observe that $|LCE(u_h)|_S$ are nonzero for $\alpha = 1/3,\, 2/5,\, 1/2$, and its convergence order is almost of 2. However, $|LCE(\widehat{u}_h)|_M$ are all of scale of 10^{-14}. Considering the errors from the linear solver, numerical quadratures and the machine precision, we can regard that $\widehat{u}_h$ satisfies the local conservation law on each control volume V_P, $P \in \mathcal{N}_h^\circ$. Moreover, we see that for all the three cases, $\widehat{u}_h$ converges to the exact solution u with optimal rates 2 and 3, respectively under H^1 and L^2 norms. These numerical results are consistent with our theoretical results in Theorem 3.2.

In comparison, we also compute the finite volume element solution u_v over eight-nodes serendipity mesh. In other words, u_v satisfies the local conservation property

$$-\int_{\partial V_P} \beta \frac{\partial u_v}{\partial \boldsymbol{n}} \,\mathrm{d}s = \int_{V_P} f \,\mathrm{d}x_1\mathrm{d}x_2$$

on each control volume V_P, $P \in \mathcal{N}_h^\circ$. The numerical results are presented in Table 4 and Table 5. One can observe that for all three cases: $\alpha = 1/3,\, 2/5,\, 1/2$, the convergence rates of H^1 errors are almost 2, which are optimal. However, the convergence rates of L^2-norm errors are also 2, which are one order lower than the optimal order.

Example 4.2. We consider the parabolic problem

$$\begin{aligned} &\frac{\partial u}{\partial t} - \nabla\cdot(\beta\nabla u) = f \qquad (x_1,x_2)\in\Omega,\ t\in(0,T], \\ &\qquad u(x_1,x_2,0) = u^0 \quad (x_1,x_2)\in\Omega, \\ &\qquad u(x_1,x_2,t) = u_D \quad (x_1,x_2)\in\partial\Omega,\ t\in(0,T] \end{aligned} \tag{13}$$

TABLE 2. Postprocess errors and convergence orders for Example 4.1, $\alpha = 2/5$.

h	$\lvert LCE(u_h)\rvert_S$	Order	$\lvert LCE(\widehat{u}_h)\rvert_M$	$\lvert u-\widehat{u}_h\rvert_1$	Order	$\lVert u-\widehat{u}_h\rVert_0$	Order
1/2	2.00e-01	/	2.44e-14	4.46e-01	/	2.19e-02	/
1/4	8.48e-02	1.235	2.86e-14	9.99e-02	2.159	2.08e-03	3.398
1/8	2.64e-02	1.682	4.67e-14	2.30e-02	2.120	1.98e-04	3.392
1/16	7.32e-03	1.852	5.48e-14	5.55e-03	2.048	2.14e-05	3.211
1/32	1.92e-03	1.928	5.19e-14	1.37e-03	2.015	2.54e-06	3.076
1/64	4.93e-04	1.964	5.72e-14	3.43e-04	2.004	3.12e-07	3.022
1/128	1.25e-04	1.982	6.19e-14	8.56e-05	2.001	3.89e-08	3.006

TABLE 3. Postprocess errors and convergence orders for Example 4.1, $\alpha = 1/2$.

h	$\lvert LCE(u_h)\rvert_S$	Order	$\lvert LCE(\widehat{u}_h)\rvert_M$	$\lvert u-\widehat{u}_h\rvert_1$	Order	$\lVert u-\widehat{u}_h\rVert_0$	Order
1/2	1.78e-01	/	2.46e-14	2.35e+00	/	1.48e-01	/
1/4	7.01e-02	1.343	3.91e-14	3.90e-01	2.591	1.21e-02	3.611
1/8	2.11e-02	1.733	5.01e-14	5.91e-02	2.723	8.78e-04	3.789
1/16	5.75e-03	1.876	5.50e-14	9.56e-03	2.627	6.31e-05	3.797
1/32	1.50e-03	1.940	5.18e-14	1.85e-03	2.371	5.08e-06	3.637
1/64	3.82e-04	1.971	5.72e-14	4.18e-04	2.144	4.99e-07	3.347
1/128	9.65e-05	1.985	6.19e-14	1.02e-04	2.043	5.71e-08	3.126

TABLE 4. FVEM H^1 errors and convergence orders for Example 4.1.

h	$\alpha = 1/3$		$\alpha = 2/5$		$\alpha = 1/2$	
	$\lvert u-u_v\rvert_1$	Order	$\lvert u-u_v\rvert_1$	Order	$\lvert u-u_v\rvert_1$	Order
1/2	2.61e-01	/	2.60e-01	/	2.58e-01	/
1/4	6.81e-02	1.936	6.77e-02	1.939	6.71e-02	1.944
1/8	1.72e-02	1.984	1.71e-02	1.985	1.69e-02	1.987
1/16	4.32e-03	1.996	4.28e-03	1.996	4.24e-03	1.997
1/32	1.08e-03	1.999	1.07e-03	1.999	1.06e-03	1.999
1/64	2.70e-04	2.000	2.68e-04	2.000	2.65e-04	2.000
1/128	6.75e-05	2.000	6.70e-05	2.000	6.63e-05	2.000

TABLE 5. FVEM L^2 errors and convergence orders for Example 4.1.

h	$\alpha = 1/3$		$\alpha = 2/5$		$\alpha = 1/2$	
	$\lVert u-u_v\rVert_0$	Order	$\lVert u-u_v\rVert_0$	Order	$\lVert u-u_v\rVert_0$	Order
1/2	2.21e-02	/	2.15e-02	/	2.07e-02	/
1/4	4.29e-03	2.363	3.96e-03	2.441	3.47e-03	2.577
1/8	9.76e-04	2.136	8.69e-04	2.189	7.02e-04	2.306
1/16	2.38e-04	2.038	2.09e-04	2.057	1.63e-04	2.105
1/32	5.90e-05	2.010	5.16e-05	2.015	4.00e-05	2.029
1/64	1.47e-05	2.003	1.29e-05	2.004	9.95e-06	2.007
1/128	3.68e-06	2.001	3.22e-06	2.001	2.48e-06	2.002

with $T = 1$ and $\beta(x_1, x_2) = e^{x_1+x_2}$. We choose the right hand side function, initial condition and boundary condition

$$f(x_1, x_2, t) = \pi e^{x_1+x_2-t}(\sin(\pi x_1)\cos(\pi x_2) + \cos(\pi x_1)\sin(\pi x_2) + 2\pi\cos(\pi x_1)\cos(\pi x_2)) - e^{-t}\cos(\pi x_1)\cos(\pi x_2),$$

TABLE 6. FVEM H^1 errors and convergence orders for Example 4.2.

h	$\alpha = 1/3$		$\alpha = 2/5$		$\alpha = 1/2$	
	$\lvert u^N - u_v^N\rvert_1$	Order	$\lvert u^N - u_v^N\rvert_1$	Order	$\lvert u^N - u_v^N\rvert_1$	Order
1/2	1.03e-01	/	1.03e-01	/	1.03e-01	/
1/4	2.07e-02	2.320	2.06e-02	2.331	2.04e-02	2.344
1/8	4.99e-03	2.054	4.93e-03	2.059	4.86e-03	2.069
1/16	1.24e-03	2.006	1.23e-03	2.007	1.21e-03	2.009
1/32	3.10e-04	2.001	3.06e-04	2.001	3.01e-04	2.001
1/64	7.75e-05	2.000	7.66e-05	2.000	7.53e-05	2.000

TABLE 7. FVEM L^2 errors and convergence orders for Example 4.2.

h	$\alpha = 1/3$		$\alpha = 2/5$		$\alpha = 1/2$	
	$\lVert u^N - u_v^N\rVert_0$	Order	$\lVert u^N - u_v^N\rVert_0$	Order	$\lVert u^N - u_v^N\rVert_0$	Order
1/2	9.80e-03	/	9.80e-03	/	9.80e-03	/
1/4	8.43e-04	3.538	8.06e-04	3.603	7.66e-04	3.677
1/8	1.82e-04	2.209	1.64e-04	2.301	1.36e-04	2.497
1/16	4.41e-05	2.048	3.88e-05	2.075	3.06e-05	2.149
1/32	1.09e-05	2.013	9.57e-06	2.021	7.43e-06	2.043
1/64	2.72e-06	2.003	2.38e-06	2.005	1.84e-06	2.011

$$u^0 = \cos(\pi x_1)\cos(\pi x_2) \quad \text{and} \quad u_D = e^{-t}\cos(\pi x_1)\cos(\pi x_2)$$

which allows the exact solution

$$u(x_1, x_2, t) = e^{-t}\cos(\pi x_1)\cos(\pi x_2).$$

In the following, we consider a uniform time step $\Delta t = 1/\lceil \frac{10}{h_k^{1.5}} \rceil$ corresponding to the mesh $\mathcal{T}_k$, where $\lceil s \rceil$ is the ceil function which rounds to the nearest integer greater than or equal to s. Set the time $t_n = n\Delta t$, $n \in \mathbb{Z}_N^0 = \{0, 1, \cdots, N\}$, where $N = \lceil \frac{10}{h_k^{1.5}} \rceil$.

We first use the Crank-Nicolson fully discrete finite volume element method over eight-nodes serendipity mesh to solve (13), i.e., find u_v^n, $n \in \mathbb{Z}_N$ which satisfies

$$\begin{aligned} &\int_{V_P} \frac{u_v^n - u_v^{n-1}}{\Delta t}\,\mathrm{d}x_1\mathrm{d}x_2 - \int_{\partial V_P} \beta\nabla\frac{u_v^n + u_v^{n-1}}{2}\cdot\boldsymbol{n}\,\mathrm{d}s \\ &= \int_{V_P} f(x_1, x_2, t_{n-\frac{1}{2}})\,\mathrm{d}x_1\mathrm{d}x_2, \quad \forall\, P \in \mathcal{N}_h^\circ, \end{aligned} \tag{14}$$

with the initial approximation $u_v^0 = I_h u^0 := \sum_{P\in\mathcal{N}_h} u^0(P)\phi_P$ and u_v^n is the finite volume element solution at time t_n, $t_{n-1/2} = (t_n + t_{n-1})/2$. The numerical results at the final time $T = 1$ are showed in Table 6 and Table 7, where $u^N = u(x_1, x_2, t_N)$. One can see that the convergence orders of H^1 errors are 2 for all three cases $\alpha = 1/3$, $2/5$, $1/2$, which are optimal. However, the convergence rates of L^2 errors are also 2, which are one order lower than the optimal convergence rate.

In order to obtain the optimal convergence order of L^2 error and satisfy the conservation, instead, we first use the Crank-Nicolson fully discrete eight-nodes serendipity finite element method to solve (13), i.e., find $u_h^n := u_h(x_1, x_2, t_n)$, $n \in$

$\mathbb{Z}_N$ which satisfies

$$\int_\Omega \frac{u_h^n - u_h^{n-1}}{\Delta t}\phi_P \,\mathrm{d}x_1\mathrm{d}x_2 + \int_\Omega \beta\nabla\frac{u_h^n + u_h^{n-1}}{2}\cdot\nabla\phi_P \,\mathrm{d}x_1\mathrm{d}x_2$$
$$= \int_\Omega f(x_1, x_2, t_{n-\frac{1}{2}})\phi_P \,\mathrm{d}x_1\mathrm{d}x_2, \quad \forall\, P \in \mathcal{N}_h^\circ,$$

with the initial approximation $u_h^0 = I_h u^0$.

Then, we postprocess u_h^n on three kinds of control volumes: $\alpha = 1/3,\ 2/5,\ 1/2$ to obtain a finite-volume-element-like solution $\widehat{u}_h^n$ which satisfies

$$\int_{V_P} \frac{\widehat{u}_h^n - \widehat{u}_h^{n-1}}{\Delta t}\,\mathrm{d}x_1\mathrm{d}x_2 - \int_{\partial V_P}\beta\nabla\frac{\widehat{u}_h^n + \widehat{u}_h^{n-1}}{2}\cdot\boldsymbol{n}\,\mathrm{d}s$$
$$= \int_{V_P} f(x_1, x_2, t_{n-\frac{1}{2}})\,\mathrm{d}x_1\mathrm{d}x_2, \quad \forall\, P \in \mathcal{N}_h^\circ,\ n \in \mathbb{Z}_N.$$

For the details of implementation, for $\forall\, n \in \mathbb{Z}_N$, suppose

$$\widehat{u}_h^n = u_h^n + \sum_{j=1}^{8} c_j^n \psi_j \text{ in each } \tau \in \mathcal{T}_h,$$

where the coefficients c_j^n, $j \in \mathbb{Z}_8$ are to be determined and ψ_j are the bubble functions defined by (4). Let the postprocessed solution $\widehat{u}_h^n$ satisfy

$$\int_{V_{P_i}\cap\tau} \frac{\widehat{u}_h^n}{\Delta t}\,\mathrm{d}x_1\mathrm{d}x_2 - \int_{(\partial V_{P_i})\cap\tau}\frac{\beta}{2}\frac{\partial\widehat{u}_h^n}{\partial\boldsymbol{n}}\,\mathrm{d}s = \widetilde{R}(f, \phi_{P_i}, \tau), \quad i \in \mathbb{Z}_8$$

for each $\tau \in \mathcal{T}_h$ and with the initial condition $\widehat{u}_h^0 = u_h^0$, where

$$\widetilde{R}(f, \phi_{P_i}, \tau)$$
$$= \int_{V_{P_i}\cap\tau} \frac{\widehat{u}_h^{n-1}}{\Delta t}\,\mathrm{d}x_1\mathrm{d}x_2 + \int_{(\partial V_{P_i})\cap\tau}\frac{\beta}{2}\frac{\partial\widehat{u}_h^{n-1}}{\partial\boldsymbol{n}}\,\mathrm{d}s$$
$$+ \int_\tau f(x_1, x_2, t_{n-\frac{1}{2}})(\phi_{P_i}^* - \phi_{P_i})\,\mathrm{d}x_1\mathrm{d}x_2 + \int_\tau \frac{u_h^n - u_h^{n-1}}{\Delta t}\phi_{P_i}\,\mathrm{d}x_1\mathrm{d}x_2$$
$$+ \int_\tau \beta\nabla\frac{u_h^n + u_h^{n-1}}{2}\cdot\nabla\phi_{P_i}\,\mathrm{d}x_1\mathrm{d}x_2 + \int_{\partial\tau}\left\{\beta\nabla\frac{u_h^n + u_h^{n-1}}{2}\right\}\cdot\boldsymbol{n}(\phi_{P_i}^* - \phi_{P_i})\,\mathrm{d}s.$$

Thus, the coefficients c_j^n, $j \in \mathbb{Z}_8$, $n \in \mathbb{Z}_N$ can be solved in each $\tau \in \mathcal{T}_h$.

On the other hand, in order to compare the LCEs of finite element solution u_h^n and its postprocessed finite-volume-element-like solution $\widehat{u}_h^n$ at time t_n, for $\forall\, v_h^n \in H^1(\Omega)$, we define the LCE associated with a control volume V_P as

$$LCE_P(v_h^n) = \int_{V_P} f(x_1, x_2, t_{n-\frac{1}{2}})\,\mathrm{d}x_1\mathrm{d}x_2 + \int_{\partial V_P}\beta\nabla\frac{v_h^n + v_h^{n-1}}{2}\cdot\boldsymbol{n}\,\mathrm{d}s$$
$$- \int_{V_P}\frac{v_h^n - v_h^{n-1}}{\Delta t}\,\mathrm{d}x_1\mathrm{d}x_2.$$

Our numerical results are presented in Tables 8-10. We observe that the convergence orders of $|LCE(u_h^N)|_S$ are almost of 2 for $\alpha = 1/3,\ 2/5,\ 1/2$. However, the $|LCE(\widehat{u}_h^N)|_M$ are almost all of scale of 10^{-15} and can be regarded as zero, i.e., $\widehat{u}_h^N$ satisfies the local conservation law on each control volume V_P, $P \in \mathcal{N}_h^\circ$. Moreover, $\widehat{u}_h^N$ converges to the exact solution u^N with optimal convergence rates 2 and 3 under H^1 and L^2 norms, namely, the convergence order of L^2 error is one order higher than the eight-nodes serendipity finite volume element method (14).

TABLE 8. Postprocess errors and convergence orders for Example 4.2, $\alpha = 1/3$.

h	$\lvert LCE(u_h^N)\rvert_S$	Order	$\lvert LCE(\widehat{u}_h^N)\rvert_M$	$\lvert u^N - \widehat{u}_h^N\rvert_1$	Order	$\lVert u^N - \widehat{u}_h^N\rVert_0$	Order
1/2	1.31e-01	/	2.89e-16	2.44e-01	/	1.63e-02	/
1/4	6.64e-02	0.982	1.45e-15	2.56e-02	3.257	4.95e-04	5.042
1/8	2.88e-02	1.205	2.04e-15	6.21e-03	2.041	4.49e-05	3.462
1/16	8.88e-03	1.700	4.22e-15	1.56e-03	1.996	5.43e-06	3.048
1/32	2.43e-03	1.866	9.01e-15	3.89e-04	2.000	6.73e-07	3.011
1/64	6.36e-04	1.937	8.39e-15	9.74e-05	2.000	8.40e-08	3.003

TABLE 9. Postprocess errors and convergence orders for Example 4.2, $\alpha = 2/5$.

h	$\lvert LCE(u_h^N)\rvert_S$	Order	$\lvert LCE(\widehat{u}_h^N)\rvert_M$	$\lvert u^N - \widehat{u}_h^N\rvert_1$	Order	$\lVert u^N - \widehat{u}_h^N\rVert_0$	Order
1/2	1.55e-01	/	1.63e-16	2.59e-01	/	1.71e-02	/
1/4	6.29e-02	1.297	1.63e-15	2.58e-02	3.325	5.24e-04	5.030
1/8	2.55e-02	1.300	2.08e-15	6.14e-03	2.071	4.64e-05	3.496
1/16	7.86e-03	1.700	4.23e-15	1.54e-03	1.996	5.63e-06	3.043
1/32	2.16e-03	1.866	9.01e-15	3.85e-04	1.999	7.00e-07	3.008
1/64	5.64e-04	1.936	8.39e-15	9.63e-05	2.000	8.74e-08	3.002

TABLE 10. Postprocess errors and convergence orders for Example 4.2, $\alpha = 1/2$.

h	$\lvert LCE(u_h^N)\rvert_S$	Order	$\lvert LCE(\widehat{u}_h^N)\rvert_M$	$\lvert u^N - \widehat{u}_h^N\rvert_1$	Order	$\lVert u^N - \widehat{u}_h^N\rVert_0$	Order
1/2	1.85e-01	/	1.51e-16	3.75e-01	/	2.32e-02	/
1/4	6.02e-02	1.616	1.45e-15	3.26e-02	3.525	7.51e-04	4.948
1/8	2.06e-02	1.548	2.12e-15	7.20e-03	2.179	6.49e-05	3.533
1/16	6.26e-03	1.718	4.21e-15	1.80e-03	1.997	7.95e-06	3.030
1/32	1.71e-03	1.870	9.01e-15	4.52e-04	1.997	9.94e-07	3.000
1/64	4.48e-04	1.936	8.39e-15	1.13e-04	1.999	1.24e-07	2.999

Example 4.3. We apply the postprocess technique to a single phase flow model in porous media. The governing equations consist of Darcy's law and a statement of conservation of mass. Neglecting the capillary pressure and gravity, the problem is

$$\nabla \cdot \boldsymbol{v} = 0 \quad (x_1, x_2) \in \Omega, \tag{15}$$

$$\frac{\partial S}{\partial t} + \nabla \cdot (\boldsymbol{v} f(S)) = 0 \quad (x_1, x_2) \in \Omega,\ t \in (0, T], \tag{16}$$

where $\boldsymbol{v} = -\beta \nabla p$ is the Darcy's velocity, β is the permeability coefficient, p is the pressure, S is the water saturation, $f(S)$ is the fractional flow function. In this example, we choose

$$\beta(x_1, x_2) = \frac{e^{1-x_1}(x_2 - x_2^2)}{1 + x_1}, \quad f(S) = S.$$

The Dirichlet boundary condition for the pressure is $p(0, x_2) = 1,\ p(1, x_2) = 0$, and the Neumann boundary condition is $\boldsymbol{v} \cdot \boldsymbol{n}(x_1, 0) = 0,\ \boldsymbol{v} \cdot \boldsymbol{n}(x_1, 1) = 0$. The boundary

condition for the saturation is $S(0, x_2, t) = 1$ and the initial condition is

$$S(x_1, x_2, 0) = \frac{1}{1 + x_1^2}.$$

Let $Y = x_2 - x_2^2$, then the true solution of saturation is [11]

$$S(x_1, x_2, t) = \begin{cases} 1, & x_1 < Yt, \\ \frac{1}{1+(x_1 - Yt)^2}, & x_1 \geq Yt. \end{cases}$$

Firstly, we use the eight-nodes serendipity finite element scheme (3) to compute the numerical solution p_h of (15), then postprocess p_h on three kinds of control volumes: $\alpha = 1/3,\ 2/5,\ 1/2$ to obtain a finite-volume-element-like solution $\widehat{p}_h$ and compute $\widehat{\boldsymbol{v}}_{\boldsymbol{h}} = -\beta \nabla \widehat{p}_h$.

Secondly, we solve (16) by finite volume method. A semi-discrete of (16) is to find the piecewise constant $S_h(x_1, x_2, t)$ with respect to each control volume V_P, $P \in \mathcal{N}_h$ such that

$$\int_{V_P} \frac{\partial S_h}{\partial t} \, \mathrm{d}x_1 \mathrm{d}x_2 + \int_{\partial V_P} \widehat{\boldsymbol{v}}_{\boldsymbol{h}} \cdot \boldsymbol{n} f(S_h) \, \mathrm{d}s = 0, \quad \forall\, P \in \mathcal{N}_h, \tag{17}$$

and $S_h(0, x_2, t) = 1$, where we have used the Green's formula on each control volume. Next, we consider a uniform time step $\Delta t = T/N$ and set the time $t_n = n\Delta t$, $n \in \mathbb{Z}_N^0$. Integrate (17) on the time interval $[t_{n-1}, t_n]$, $n \in \mathbb{Z}_N$, and use the left end point quadrature rule to the second term, we arrive at the fully discrete of (16) is to find $S_h(x_1, x_2, t_n)$, $n \in \mathbb{Z}_N$ such that

$$meas(V_P)(S_h(P, t_n) - S_h(P, t_{n-1})) + \Delta t \int_{\partial V_P} \widehat{\boldsymbol{v}}_{\boldsymbol{h}} \cdot \boldsymbol{n} f(S_h(t_{n-1})) \, \mathrm{d}s = 0, \ \forall\, P \in \mathcal{N}_h, \tag{18}$$

and $S_h(0, x_2, t_n) = 1$, where $meas(V_P)$ is the measure of V_P and $S_h(P, t_0) = S(P, 0)$. In other words, the saturation $S_h(t_n)$ in (18) can be explicitly solved by $S_h(t_{n-1})$ and do not need to solve the system of linear equations. Since $S_h(t_{n-1})$ is discontinuous on $\partial V_P \backslash \partial\Omega$ in the second term of (18), we apply the widely used upwind scheme to decide the appropriate value of $f(S_h(t_{n-1}))$, see [7, 11, 30] for details.

The numerical results of the postprocessing are presented in Tables 11-13, where $N = 500$ and $T = 0.01$, $S^N = S(x_1, x_2, t_N)$ and $S_h^N = S_h(x_1, x_2, t_N)$ are the exact saturation and numerical saturation at the final time T respectively. One can see that the convergence orders of $|LCE(p_h)|_S$ are almost of 2 for $\alpha = 1/3,\ 2/5,\ 1/2$. However, the $|LCE(\widehat{p}_h)|_M$ are almost all of scale of 10^{-15}, namely, the local conservation property holds for $\widehat{p}_h$. On the other hand, the postprocessed solution $\widehat{p}_h$ converges to the finite element solution p_h with optimal convergence rate 3 under L^2 norm. These numerical results are validate the theoretical findings in Theorem 3.2. Moreover, the numerical saturation S_h^N converges to the true saturation S^N with optimal convergence order 1 under L^2 norm.

In comparison, we also compute the finite volume element solution p_h^v of (15) over eight-nodes serendipity mesh. The numerical results are reported in Table 14. One can observe that for all three cases: $\alpha = 1/3,\ 2/5,\ 1/2$, the convergence rates of L^2-norm errors are 2, which are one order lower than the optimal convergence order.

5. Conclusion

Comparing to the theory of finite element method, that of the finite volume element method has not been developed maturely on dealing with the high order schemes over serendipity meshes. In this work, we derive a locally conservative

TABLE 11. Postprocess errors and convergence orders for Example 4.3, $\alpha = 1/3$.

h	$\|LCE(p_h)\|_S$	Order	$\|LCE(\widehat{p}_h)\|_M$	$\|p_h - \widehat{p}_h\|_0$	Order	$\|S^N - S_h^N\|_0$	Order
1/2	2.35e-03	/	1.54e-13	2.08e-03	/	4.92e-02	/
1/4	7.12e-04	1.726	8.40e-16	2.71e-04	2.938	2.48e-02	0.988
1/8	1.92e-04	1.891	1.52e-15	3.41e-05	2.988	1.24e-02	0.997
1/16	4.95e-05	1.956	2.29e-15	4.27e-06	2.999	6.23e-03	0.997
1/32	1.25e-05	1.981	4.88e-15	5.33e-07	3.001	3.13e-03	0.991
1/64	3.15e-06	1.991	8.68e-15	6.66e-08	3.001	1.59e-03	0.976

TABLE 12. Postprocess errors and convergence orders for Example 4.3, $\alpha = 2/5$.

h	$\|LCE(p_h)\|_S$	Order	$\|LCE(\widehat{p}_h)\|_M$	$\|p_h - \widehat{p}_h\|_0$	Order	$\|S^N - S_h^N\|_0$	Order
1/2	2.59e-03	/	1.48e-13	2.21e-03	/	4.72e-02	/
1/4	7.82e-04	1.729	9.78e-16	2.90e-04	2.931	2.38e-02	0.989
1/8	2.11e-04	1.888	1.37e-15	3.65e-05	2.991	1.19e-02	0.997
1/16	5.45e-05	1.954	3.19e-15	4.55e-06	3.003	5.97e-03	0.997
1/32	1.38e-05	1.980	4.39e-15	5.68e-07	3.003	3.00e-03	0.993
1/64	3.48e-06	1.991	8.10e-15	7.08e-08	3.002	1.52e-03	0.982

TABLE 13. Postprocess errors and convergence orders for Example 4.3, $\alpha = 1/2$.

h	$\|LCE(p_h)\|_S$	Order	$\|LCE(\widehat{p}_h)\|_M$	$\|p_h - \widehat{p}_h\|_0$	Order	$\|S^N - S_h^N\|_0$	Order
1/2	2.71e-03	/	1.27e-13	2.73e-03	/	4.63e-02	/
1/4	8.26e-04	1.712	9.71e-16	3.66e-04	2.898	2.33e-02	0.991
1/8	2.24e-04	1.885	1.33e-15	4.52e-05	3.019	1.17e-02	0.998
1/16	5.78e-05	1.952	3.20e-15	5.55e-06	3.025	5.84e-03	0.998
1/32	1.47e-05	1.979	3.98e-15	6.86e-07	3.016	2.93e-03	0.996
1/64	3.69e-06	1.990	7.57e-15	8.53e-08	3.009	1.48e-03	0.988

TABLE 14. FVEM L^2 errors and convergence orders of pressure p for Example 4.3.

h	$\alpha = 1/3$		$\alpha = 2/5$		$\alpha = 1/2$	
	$\|p_h^v - p_{\frac{h}{2}}^v\|_0$	Order	$\|p_h^v - p_{\frac{h}{2}}^v\|_0$	Order	$\|p_h^v - p_{\frac{h}{2}}^v\|_0$	Order
1/2	1.80e-03	/	1.77e-03	/	1.73e-03	/
1/4	2.45e-04	2.876	2.38e-04	2.893	2.28e-04	2.920
1/8	3.77e-05	2.699	3.54e-05	2.746	3.22e-05	2.823
1/16	7.22e-06	2.385	6.52e-06	2.443	5.46e-06	2.560
1/32	1.64e-06	2.141	1.45e-06	2.172	1.15e-06	2.252
1/64	3.98e-07	2.040	3.49e-07	2.050	2.71e-07	2.080
1/128	9.88e-08	2.010	8.65e-08	2.013	6.69e-08	2.021

solution with global continuity by postprocessing an eight-nodes-serendipity finite element solution of the prescribed elliptic equation, and theoretically show that our postprocessed solution converges to the exact solution with optimal convergence orders under both H^1 and L^2 norms. Moreover, several numerical examples are

presented to verify our theoretical results. In future, we expect to apply our post-processing technique to study other serendipity finite element solutions.

Acknowledgments

This research was supported in part by the special project High Performance Computing of National Key Research and Development Program 2016YFB0200604, NSFC Grant 12071496, Guangdong Provincial NSF Grant 2017B030311001.

References

[1] Ahmad, S.: Curved finite elements in the analysis of solid, shell, and plate structures. PhD Thesis, University of Wales, Swansea, UK (1969).
[2] Arnold, D., Awanou, G.: The serendipity family of finite elements. Found. Comput. Math., 11, 337-344 (2011).
[3] Arnold, D., Boffi, D., Falk, R.: Approximation by quadrilateral finite elements. Math. Comput., 71, 909-922 (2002).
[4] Barth, T., Ohlberger, M.: Finite Volume Methods: Foundation and Analysis. In: Encyclopedia of Computational Mechanics, vol. 1, chapter 15. Wiley (2004).
[5] Braess, D.: Finite Elements: Theory, Fast Solvers, and Applications in Solid Mechanics, 3rd ed. Cambridge University Press (2007).
[6] Brenner, S., Scott, L.: The mathematical theory of finite element methods, 3rd ed. Texts in Applied Mathematics, Springer (2008).
[7] Bush, L., Ginting, V.: On the application of the continuous Galerkin finite element method for conservation problems. SIAM J. Sci. Comput., 35, A2953-A2975 (2013).
[8] Chen, Z., Wu, J., Xu, Y.: Higher-order finite volume methods for elliptic boundary value problems. Adv. Comput. Math., 37, 191-253 (2012).
[9] Chen, Z., Xu, Y., Zhang, Y.: A construction of higher-order finite volume methods. Math. Comp., 84, 599-628 (2015).
[10] Ciarlet, P.: The finite element method for elliptic problems. North-Holland, Amsterdam (1978).
[11] Deng, Q., Ginting, V.: Locally conservative continuous Galerkin FEM for pressure equation in two-phase flow model in subsurfaces. J. Sci. Comput., 74, 1264-1285 (2018).
[12] Fu, X., Cen, S., Li, C., Chen, X.: Analytical trial function method for development of new 8-node plane element based on the variational principle containing Airy stress function. Eng. Computations, 25, 442-463 (2010).
[13] Gong, W., Zou, Q.: Locally conservative finite element solutions for parabolic equations. Int. J. Numer. Anal. Mod., 5, 679-694 (2020).
[14] Hong, Q., Wu, J.: A Q_1-finite volume element scheme for anisotropic diffusion problems on general convex quadrilateral mesh. J. Comput. Appl. Math., 372, 112732 (2020).
[15] Kikuchi, F.: Explicit expressions of shape functions for the modified 8-node serendipity element. Com. Num. Meth. Eng., 10, 711-716 (1994).
[16] Kikuchi, F., Okabe, M., Fujio, H.: Modification of the 8-node serendipity element. Comput. Methods Appl. Mech. Engrg., 179, 91-109 (1999).
[17] Lee, N., Bathe, K.: Effects of element distortion on the performance of isoparametric elements. Int. J. Numer. Meth. Eng., 36, 3553-3576 (1993).
[18] LeVeque, R. J.: Finite Volume Methods for Hyperbolic Problems. Cambridge Texts in Applied Mathematics. Cambridge University Press, Cambridge (2002).
[19] Li, L., Kunimatsu, S., Han, X., Xu, S.: The analysis of interpolation precision of quadrilateral elements. Finite Elem. Anal. Des., 41, 91-108 (2004).
[20] Li, R., Chen, Z., Wu, W.: The Generalized Difference Methods for Partial Differential Equations: Numerical Analysis of Finite Volume Methods. Marcel Dikker, New York (2000).
[21] Li, Y., Li, R.: Generalized difference methods on arbitrary quadrilateral networks. J. Comput. Math., 17, 653-672 (1999).
[22] Lin, Y., Liu, J., Yang, M.: Finite volume element methods : an overview on recent developments. Int. J. Numer. Anal. Mod. B, 4, 14-34 (2013).
[23] Lin, Y., Yang, M., Zou, Q.: L^2 error estimates for a class of any order finite volume schemes over quadrilateral meshes. SIAM J. Numer. Anal., 53, 2030-2050 (2015).
[24] Lv, J., Li, Y.: L^2 error estimates and superconvergence of the finite volume element methods on quadrilateral meshes. Adv. Comput. Math., 37, 393-416 (2012).

[25] Lv, J., Li, Y.: Optimal biquadratic finite volume element methods on quadrilateral meshes. SIAM J. Numer. Anal., 50, 2379-2399 (2012).
[26] MacNeal, R., Harder, R.: Eight nodes or nine ? Int. J. Numer. Meth. Eng., 33, 1049-1058 (1992).
[27] Moukalled, F., Mangani, L., Darwish, M.: The Finite Volume Method in Computational Fluid Dynamics: An Advanced Introduction with OpenFoam and Matlab, Springer, Switherland (2016).
[28] Rajendran, S., Liew, K. M.: A novel unsymmetric 8-node plane element immune to mesh distortion under a quadratic displacement field. Int. J. Numer. Meth. Eng., 58, 1713-1748 (2003).
[29] Rand, A., Gillette, A., Bajaj, C.: Quadratic serendipity finite elements on polygons using generalized barycentric coordinates. Math. Comput., 83, 2691-2716 (2014).
[30] Thomas, J. W.: Numerical Partial Differential Equations: Conservation Laws and Elliptic Equations, vol. 33, Springer Science & Business Media, Berlin (2013).
[31] Versteeg, H. K., Malalasekra, W.: An Introduction to Computational Fluid Dynamics: the Finite Volume Method, 2nd ed. Pearson Education, England (2007).
[32] Wang, X., Li, Y.: L^2 error estimates for high order finite volume methods on triangular meshes. SIAM J. Numer. Anal., 54, 2729-2749 (2016).
[33] Xu, J., Zou, Q.: Analysis of linear and quadratic simplicial finite volume methods for elliptic equations. Numer. Math., 111, 469-492 (2009).
[34] Yang, M.: A second-order finite volume element method on quadrilateral meshes for elliptic equations. ESAIM: M2AN, 40, 1053-1067 (2006).
[35] Zhang, J., Kikuchi, F.: Interpolation error estimates of a modified 8-node serendipity finite element. Numer. Math., 85, 503-524 (2000).
[36] Zhang, Z., Zou, Q.: Some recent advances on vertex centered finite volume element methods for elliptic equations. Sci. China Math., 56, 2507-2522 (2013).
[37] Zhang, Z., Zou, Q.: Vertex-centered finite volume schemes of any order over quadrilateral meshes for elliptic boundary value problems. Numer. Math., 130, 363-393 (2015).
[38] Zhou, Y.: A class of bubble enriched quadratic finite volume element schemes on triangular meshes. Int. J. Numer. Anal. Mod., 17, 872-899 (2020).
[39] Zhou, Y., Wu, J.: A family of quadratic finite volume element schemes over triangular meshes for elliptic equations. Comput. Math. Appl., 79, 2473-2491 (2020).
[40] Zhou, Y., Wu, J.: A unified analysis of a class of quadratic finite volume element schemes on triangular meshes. Adv. Comput. Math., 46, 71 (2020).
[41] Zienkiewicz, O. C.: The Finite Element Method, 3rd revised edn. McGraw-Hill, London (1977).
[42] Zou, Q.: An unconditionally stable quadratic finite volume scheme over triangular meshes for elliptic equations. J. Sci. Comput., 70, 112-124 (2017).
[43] Zou, Q., Guo, L., Deng, Q.: High order continuous local-conserving fluxes and finite-volume-like finite element solutions for elliptic equations. SIAM J. Numer. Anal., 55, 2666-2686 (2017).

School of Data and Computer Science, Sun Yat-Sen University, Guangzhou, 510275, China
E-mail: zhouyh9@mail2.sysu.edu.cn

Corresponding author. School of Data and Computer Science and Guangdong Province Key Laboratory of Computational Science, Sun Yat-Sen University, Guangzhou, 510275, China
E-mail: mcszqs@mail.sysu.edu.cn